中国科学: 地球科学 2023 年 第 53 卷 第 9 期: 2059 ~ 2071
SCIENTIA SINICA Terrae earthcn.scichina.com
《中国科学》杂志社 SCIENCE CHINA PRESS
CrossMark click for updates

论 文

晚中生代-新生代亚洲砂岩型铀矿幕式大爆发

张闯*

中国核工业集团公司, 核工业北京地质研究院, 北京 100029
* 通讯作者, E-mail: zhangc198506@126.com

收稿日期: 2022-05-09; 收修改稿日期: 2023-03-02; 接受日期: 2023-04-03; 网络版发表日期: 2023-07-19
中国核工业集团公司铀矿科研项目(编号: 22045004、QNYC2103)资助

摘要 砂岩型铀矿床是全球最重要的铀供给源, 但尚不清楚它们在时间和空间上为什么非随机分布. 一般认为, 砂岩型铀矿床是由砂岩中的地下水循环而形成. 地下水通常来源于区域性降水, 具有氧化性特征, 表明区域气候可能在砂岩型铀矿床的形成中起到关键作用. 此外, 地下水循环受盆地演化的影响, 这意味着区域构造运动也可能控制砂岩型铀矿床的形成. 本文汇编了亚洲的砂岩型铀矿床, 系统梳理了已经报道的砂岩型铀矿床年龄数据, 并将其与主要砂岩型铀矿集区的隆升历史及亚洲晚中生代-新生代气候演化进行了综合对比分析. 结果表明, 除了外乌拉尔地区的一些砂岩型铀矿床外, 亚洲大多数砂岩型铀矿床形成于晚白垩世至第四纪, 可分为三个阶段: 晚白垩世-古近纪早期(80~50Ma; 第一阶段)、渐新世-中新世中期(25~17Ma; 第二阶段)和中新世晚期-现在(8~0Ma; 第三阶段). 对比分析结果表明, 亚洲砂岩型铀矿床的形成与印度-欧亚大陆碰撞、太平洋板块俯冲、温室气候阶段湿度增加和亚洲季风强度加剧有密切关系.

关键词 砂岩型铀矿床, 印度-欧亚大陆碰撞, 亚洲季风, 亚洲西风

1 引言

砂岩型铀矿床约占全球铀资源储量的30%, 占全球铀产量的50%以上(Cheng等, 2019; Jin等, 2020), 但该类型矿床的形成时代与产出位置并非随机分布(Groves等, 2005; Robb, 2005; 程银行等, 2020; Cheng等, 2020). 大多数砂岩型铀矿床产于北半球25°~50°N的中新生代盆地中, 多形成于晚中生代-新生代(Dahlkamp, 2009, 2010, 2016; OECD-NEA/IAEA, 2014). 一般认为, 砂岩型铀矿床是由砂岩(即碎屑沉积物)中的地下水循环而形成(Phillips和Castro, 2014; 金若时等, 2017), 这些水通常与区域性降水密切相关, 具有氧化性特征(Pagel等, 2005), 意味着区域气候可能在铀矿化中起到关键作用. 地下水循环受盆地演化的影响, 表明区域构造运动可能也控制了砂岩型铀矿床的形成(Cuney, 2010). 因此, 构造作用和气候可能是导致砂岩型铀矿床非随机性分布的重要因素. 在本研究中, 作者汇编了亚洲的砂岩型铀矿集区(图1), 系统梳理了这些砂岩型铀矿集中区已经报道的年龄数据, 在必要时检验并重新计算已发表的年龄数据(Ludwig等, 1984, 1985; Ludwig, 1993), 并将这些矿床形成年龄与区域上的隆升历史、亚洲晚中生代-新生代气候演化进行了系统对比分析.

中文引用格式: 张闯. 2023. 晚中生代-新生代亚洲砂岩型铀矿幕式大爆发. 中国科学: 地球科学, 53(9): 2059–2071, doi: 10.1360/N072022-0136
英文引用格式: Zhang C. 2023. Episodic sandstone-type uranium mineralization in Asia during the Late Mesozoic-Cenozoic. Science China Earth Sciences, 66(9): 2034–2044, https://doi.org/10.1007/s11430-022-1096-8

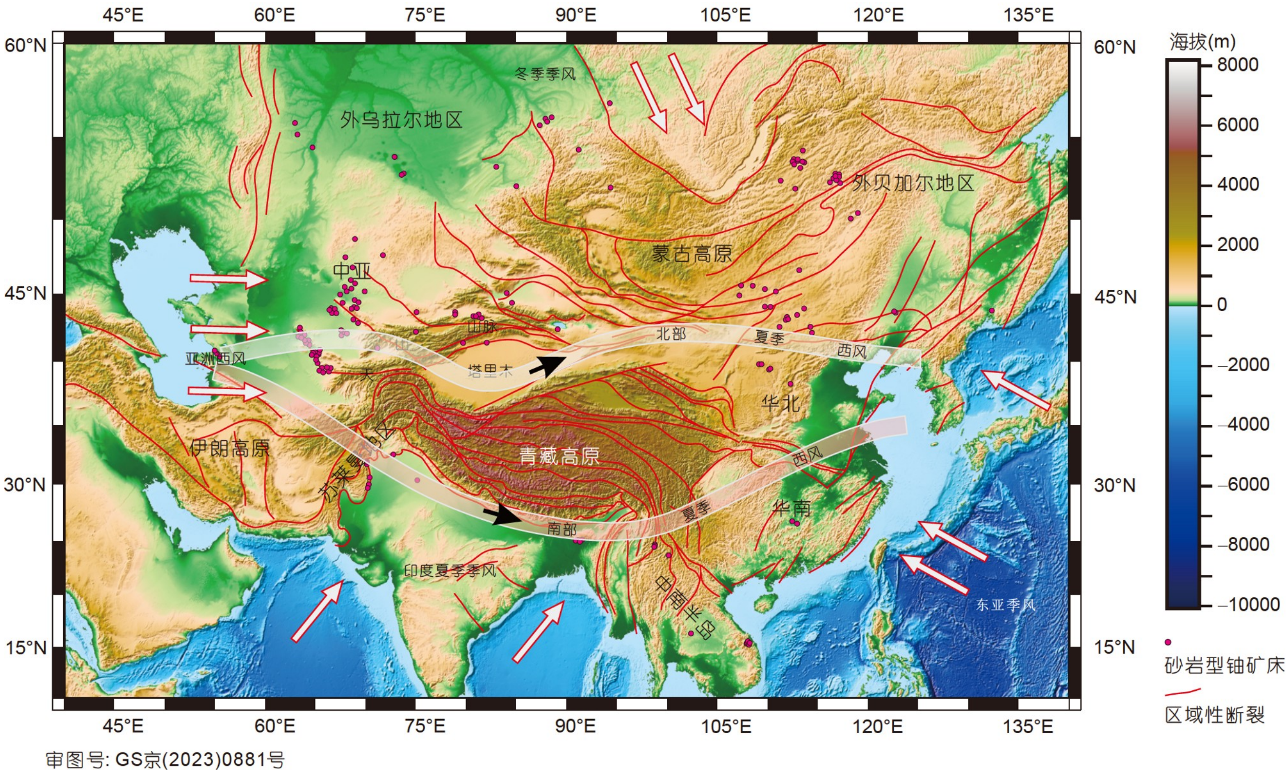

图 1　亚洲地形和构造示意图

图中显示了主要砂岩型铀矿集区的构造位置和主要气候特征, 季风模式参考Aizen等(2001)和Chen等(2019)

2　地质与气候背景

亚洲地区砂岩型铀矿床主要分布在四个地区: 中亚-外乌拉尔地区、华北-外贝加尔地区、华南-中南半岛和印度北部-苏莱曼山脉, 少量分布于里海地区和日本(图1). 这些砂岩型铀矿床通常产出于大陆河流相或滨海相(即河流-海洋交界)沉积物中(网络版附表S1, http://earthcn.scichina.com; 例如, Petrov, 1998; Petrov等, 2000; Fyodorov, 2002a, 2002b; Zhang和Liu, 2019). 矿床多产出于中-新生代前陆盆地(如印度北部的Meghalaya高原)或山间盆地(如中国西北部的伊犁和吐哈盆地; Burtman, 1975). 这些砂岩型铀矿床被认为是晚中生代-新生代欧亚大陆内部构造运动的结果. 而这些构造运动则是印度-欧亚大陆碰撞和太平洋板块俯冲的共同结果(Molnar和Tapponnier, 1975; Tapponnier等, 1982; Davy和Cobbold, 1988; Fournier等, 2004). 印度-欧亚大陆碰撞和太平洋板块俯冲导致形成了喜马拉雅山脉与青藏高原, 再度激活了天山和阿尔泰山山脉, 使蒙古高原开始了再次隆升, 并导致了亚洲内部众多盆地的形成与发展(例如, Yin, 2010; Li等, 2012a, 2012b).

前人已经通过地质、古生物、气候建模等多种手段, 系统重塑了亚洲地区的气候演化历史(例如, Boucot等, 2013; 金若时等, 2017; Jin等, 2022). 晚白垩世, 东亚与北亚地区盛行大规模季风环流(Yapp和Poths, 1996; Bice和Norris, 2002), 中国陆地大部分位于半干旱气候带. 而东北亚, 尤其靠近西太平洋的地区, 其降水量可能很大, 年平均降水量可达1200mm/a(约66Ma; Gao等, 2015). 这种气候环境一直持续到古新世早期(约60Ma; Hong等, 2018). 新生代早期, 全球范围内的气候波动对亚洲地区的影响强烈(例如, Zachos等, 2001; Hong等, 2018), 东亚植被和Pelobatoidea分布表明, 该地区温暖湿润(平均年降水量约为800~1400mm/a; Chen X Q等, 2015; Zhang等, 2016). 自始新世以来, 季风-干旱气候系统在亚洲变得越来越重要(Gu和Renaut, 1994; Clemens, 2006; Huber和Goldner, 2012), 并且自

渐新世晚期开始处于主导地位(Sun和Wang, 2005; Guo等, 2008; Jiang和Ding, 2008; Jiang等, 2008). 至上新世, 当今亚洲季风-干旱气候系统的气候模式才完全确立(An等, 2001, 2014), 此时, 亚洲陆内的盆地中开始形成众多的砂岩型铀矿床(Zhang等, 2018; Zhang和Liu, 2019).

3 分析方法与结果

前人已经对亚洲域内的砂岩型铀矿床进行了大量地质年代学研究(例如, Dahlkamp, 2009; 夏毓亮, 2019). 最近的铀矿床年代学研究开始采用沥青铀矿的微区原位测年方法(Alexandre等, 2007, 2012; Bonnetti等, 2018). 然而, 砂岩型铀矿床中沥青铀矿的矿物学特征与该方法中常见的锆石差异巨大(例如, Bowring等, 1998; Thomas, 2011), 且沥青铀矿中普遍存在普通铅过量及铀衰变子体扩散等现象(Faure, 1977; Rollinson, 1994; Fayek等, 2000). 这些现象的存在都会最终影响年代学研究的可靠性.

为了最大限度地减少这些现象对铀矿年代学研究的影响, 部分研究者认为全岩U-Pb定年法可能更为可靠. 该方法采用体积相对较大的样品(>1kg)(Ludwig, 1978). 然而, 该方法受到初始铅同位素组成不均一、碎屑矿物少量存在等因素的影响, 容易造成误差较大, 使最终给出的等时线年龄具有相对较大的误差(Davis等, 2003). 可采用铅同位素综合分析, 评估初始铅同位素组成的均一性, 以及矿石中铀和(或)放射性衰变子体的损失和(或)添加(Ludwig等, 1981, 1984; Ludwig和Simmons, 1992), 从而帮助筛选和剔除异常数据. 剔除异常数据后(Zhang等, 2018; Zhang和Liu, 2019), $^{238}U/^{204}Pb-^{206}Pb/^{204}Pb$和$^{235}U/^{204}Pb-^{207}Pb/^{204}P$的线性趋势表明, 全岩U-Pb等时线法所获得的年龄是可靠的. 中亚(包括俄罗斯)、印度和中南半岛砂岩型铀矿床的全岩U-Pb年龄原始数据并未找到. 中国境内所报道的砂岩型铀矿床年龄差异很大, 但是伊犁、准噶尔、吐哈、鄂尔多斯、松辽和额仁盆地中砂岩型铀矿床年代学研究的原始U-Pb数据可用(附表S1). 作者重新梳理了前人发布的数据, 并对这些数据进行了再次计算(参考: Ludwig, 1978, 1980, 1984, 1993), 从而获得了这些砂岩型铀矿床的可靠成矿年龄.

除了乌拉尔地区的少数砂岩型铀矿床外, 亚洲域内大多数砂岩型铀矿床形成于晚白垩世至第四纪, 可分为三个主要阶段: 晚白垩纪-古近纪早期(80~50Ma; 阶段Ⅰ)、渐新世-中新世中期(25~17Ma; 阶段Ⅱ)和中新世晚期-现在(8~0Ma; 阶段Ⅲ)(附表S1; 图2). 外乌拉尔地区矿化年龄为340~370Ma和~135Ma的砂岩型铀矿床不在分析之列. 因为对于这些时期外乌拉尔地区的气候环境研究较为缺乏. 相比之下, 晚白垩世至第四纪, 亚洲的构造演化、区域隆升和气候演化则已相当深入(例如, An等, 2001; Clift等, 2014; Clift和Webb, 2019).

4 讨论

地质年代学数据分析表明, 对于特定的砂岩型铀矿集区, 通常会存在两个或两个以上的铀成矿阶段, 如鄂尔多斯北缘铀集中区(例如, 65~60Ma和~25Ma; Zhang等, 2018)和中亚铀成矿省(例如, 25~22Ma和0.25~0.10Ma; Dahlkamp, 2009; 图2b~2f). 产出砂岩型铀矿床的盆地尽管相距数千公里(图1), 但其中的砂岩型铀矿床具有相似的成矿年龄, 如Chu-Sarysu和Syr-Darya盆地中的砂岩型铀矿床形成于25~22Ma, 中亚伊犁铀矿集区形成于23~17Ma, 印度北部Meghalaya高原铀矿集区形成于约25Ma, 以及中国北部鄂尔多斯盆地铀矿集区形成于25~22Ma(附表S1). 这说明, 在亚洲全域内, 适合砂岩型铀矿产出的构造与气候背景在晚古生代-新生代这一时期内反复出现. 砂岩型铀矿床的形成通常被认为是地表水向砂岩中渗入所导致的(Cuney和Kyser, 2008), 这就要求: (1) 含矿砂岩的一端暴露在地表; (2) 存在大量的地表氧化水; (3) 地下水的运移通道流畅(Phillips和Castro, 2014). 砂岩地层的端元出露通常与盆缘的隆升剥蚀有关. 而剥蚀作用又与地表的大量降水关系密切, 因为大范围降水是地表碎屑物质从隆起区搬运至沉积区的前提(Koons等, 2002; Malavieille, 2010). 这一过程可以将盆缘深埋的砂岩地层带至地表, 从而创造向砂岩地层中注入大量氧化地表水的条件. 构造作用通常导致砂岩地层的差异抬升和倾斜. 不同位置砂岩地层的高程差是地下水循环的重要驱动力(Phillips和Castro, 2014). 而丰富的大气降水往往指示潮湿的气候背景.

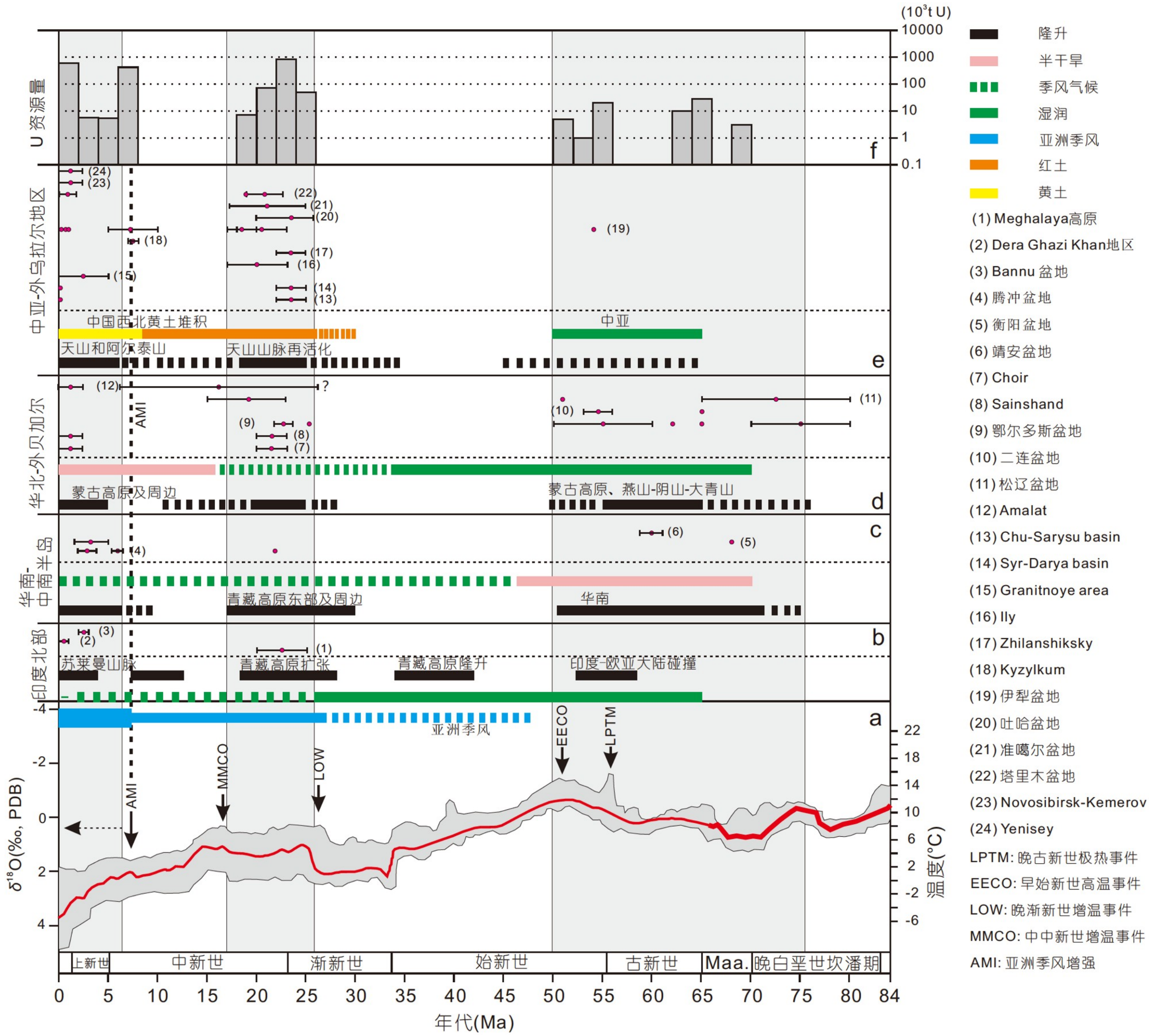

图 2　晚中生代-新生代亚洲主要构造事件、全球与亚洲气候演化、区域隆升、砂岩型铀成矿综合对比分析示意图

(a) 晚白垩世至今底栖有孔虫演化的稳定氧同位素汇编(84Ma至今; Friedrich等, 2012)与全球海水温度(Zachos等, 2001); (b) 印度北部主要砂岩型铀成矿、区域隆起事件、晚白垩世至全新世期间主要气候事件; (c) 华南-中南半岛主要砂岩型铀矿化、区域隆起事件、晚白垩世至全新世期间主要气候事件; (d) 华北-外贝加尔主要砂岩型铀矿化、区域隆起事件、晚白垩世至全新世期间主要气候事件; (e) 中亚-外贝加尔主要砂岩型铀矿化、区域隆起事件、晚白垩世至全新世期间主要气候事件; (f) 亚洲砂岩型铀矿资源量时间分布. Maa.代表晚白垩世马斯特里赫特期

4.1　成矿第一阶段

亚洲域内的第一阶段砂岩型大规模铀成矿(晚白垩世-古近纪早期)主要发生在亚洲东部, 以中国的华北和华南地区为主. 晚白垩世, 东亚地区处于从伸展构造环境向挤压构造环境过渡的阶段(例如, 柳益群等, 2009; Yang, 2013). 这一时期, 华北-外贝加尔地区主要表现为蒙古高原和华北板块中北部的沉积停止, 并开始经历大范围的区域隆升(例如, Zhang等, 2011; 附表S2). 相比之下, 在晚白垩世(~78Ma以来), 中国华南地区开始经历南北向伸展, 区域上主要表现为差异隆升和山间盆地的形成(Li等, 2014a, 2014b), 该伸展作用一直持续至古近纪早期(Zhang等, 2012; Mercier等, 2013; 附表S2). 此时, 在气候方面, 东亚地区被大

规模季风环流所控制(Yapp和Poths, 1996; Bice和Norris, 2002), 欧亚大陆上空的大气环流系统呈现出强烈的经向特征. 滨太平洋地区的陆地可能经历更多降水, 降水量超过1200mm/a. 自~34Ma以来, 随着全球气温的降低(图2a), 华北-外贝加尔地区可能变得更加干燥(Clift和Webb, 2019). 在降温期间, 该区域主要受极地高压气团控制, 从而阻挡了来自太平洋的暖湿空气(Crumley, 2004; Hong等, 2018), 使该地区处于干旱环境.

区域构造演化与气候条件影响和制约着砂岩型铀矿床的形成. 华南地区的砂岩型铀矿床(Ⅰ期)主要为潜水氧化面亚型, 赋矿围岩主要为红色岩层(中国核工业地质局和核工业北京地质研究院, 2010; 姜必广等, 2017); 矿体多受地层产状控制, 呈板状或透镜状, 少量为卷状矿体; 矿体的长度和宽度从20~200m不等, 大部分厚度为0.5~1.0m, 埋深为10~200m不等(黄净白等, 2005); 单个矿床的铀资源量通常小于3000吨; 铀主要呈吸附态, 产于有机质和黏土之中, 部分呈沥青铀矿和铀钍石(Dahlkamp, 2009). 相比之下, 华北-外贝加尔地区的砂岩型铀矿床主要为卷状和板状亚型, 赋矿围岩为细粒至粗粒砂岩, 富含碳质碎屑和油气(韩效忠等, 2008; Dahlkamp, 2009); 铀矿体长数十至数百米, 厚度1~20m, 平均品位为0.02~0.1%(重量)铀; 单个矿床的铀资源量可达10000吨; 铀通常以铀钍石和沥青铀矿的形式存在, 吸附在黏土矿物上的相对较少(Dahlkamp, 2009; Zhang等, 2018).

在第一阶段, 全球正在经历极端的变暖事件, 如古新世-始新世热极事件(PETM)和早始新世气候变暖事件(EECO). 在这些事件中, 表层海水温度升高4~9℃. 这些增温事件会大大增加海洋蒸发和全球范围内的降水量(例如, Raymo和Ruddiman, 1992; Anagnostou等, 2016; 图2a). 在这些全球变暖事件的背景下, 华北-外贝加尔地区表现为相对湿润的气候环境, 地表发育大量沼泽(Chen等, 2016). 该气候变暖正好对应中国境内大规模砂岩型铀矿的形成, 例如, 华南的靖安盆地(铀矿床年龄: 61~51Ma)、鄂尔多斯(铀矿床年龄: 60~50Ma)、中国北部的额仁(铀矿床年龄: 56~53Ma)和松辽盆地(铀矿床年龄: 50Ma)以及中国新疆伊犁盆地的红海沟矿床(54Ma). 这表明, 第一阶段砂岩型铀矿床的形成受到这些变暖事件的显著影响. 此外, 这些地区正在经历大范围的差异隆升. 而这些区域隆升事件又受太平洋板块与特提斯洋板块向欧亚大陆下俯冲的控制(附表S2). 盆地边缘的构造抬升和降水量的增加共同导致了这些地区砂岩型铀矿床的形成.

4.2　成矿第二阶段

第二阶段(晚渐新世~中中新世)的砂岩型铀矿化在亚洲广泛发育, 在四个主要地区几乎同时发生. 晚渐新世至早中新世, 亚洲地区最重要的构造事件是喜马拉雅山脉的快速隆升. 该事件发生自~25Ma以来, 与印度板块向欧亚大陆下方的俯冲作用直接相关(Catlos等, 2001; Clift和Webb, 2019). 在此期间, 青藏高原经历了快速扩张(Wang C S等, 2014). 自此, 亚洲主体构造及地形格局形成(An等, 2014), 东-西向天山(中亚)因印度-欧亚碰撞的远程效应而被重新激活(Liu等, 2017). 前人依据磷灰石裂变径迹数据和山间盆地的沉积历史(郭召杰等, 2006; Buslov等, 2008), 推断天山在25~18Ma(>2000m, 28~17Ma; 张文高和陈正乐, 2017)经历了快速隆升剥蚀. 与此同时, 中国华北北部及其周围山脉经历了快速冷却(25~23Ma; 王同和等, 2001; Cao等, 2015). 这一热冷却事件被认为与青藏高原向东北方向的增生有关(Yin, 2010; Chen K等, 2015). 这些快速隆升事件在区域沉积学研究中清晰可见, 如中亚一些山间盆地中, 上新世地层不整合覆盖在白垩系之上(Harrison等, 1992; Wang等, 2015). 青藏高原向东的生长导致中国华南的区域性伸展停止, 并使华南和中南半岛在晚渐新世至早中新世经历快速隆升剥蚀(例如, Zhang等, 2012; Mercier等, 2013). 该阶段, 中国西南的腾冲盆地边缘开始经历隆升与剥蚀(陶君容和杜乃秋, 1982).

自早中新世开始, 亚洲季风-干旱气候系统形成(An等, 2014). 大气分析和全球气候模拟表明, 在新生代的大部分时间里, 中亚地区60%以上的水分由亚洲西风输送(Curio等, 2015; Caves, 2017). 天山的隆起阻挡了亚洲西风带向中国西北地区的水汽输送, 导致天山及其周边变得更加湿润(Caves等, 2017). 由于降水差异, 天山山脉西部-北部侧翼比东部-南部侧翼更加湿润(即背风侧; Meyer-Christoffer等, 2015; Caves, 2017). 同时, 天山山脉的西部和北部侧翼将经历更大程度的剥蚀(Charreau等, 2005, 2006, 2009), 这导致大量降水在重力作用下注入盆缘出露的砂岩地层. 西北地区降水量的大幅度减少可能始于约25Ma, 这与天山

山脉的快速隆升相对应. 因此, 中国内陆的大规模黄土沉积自此时开始(约22Ma之前; Sun和Windley, 2015).

中亚第二阶段的砂岩型铀矿化大致发生于25~17Ma, 高峰期在25~20Ma(图2f; 附表S1). 其形成时间正好对应天山山脉的快速隆起(例如, 陈正乐等, 2008; 吕红华等, 2008a, 2008b, 2013)和中亚地区的气候演变(例如, Sato等, 2007; Roe等, 2016; Caves, 2017). 天山隆起与中亚地区的气候演变联合导致了中亚大规模砂岩型铀矿床的形成. 由西风带所输入的大气降水注入天山山脉北部和西部的砂岩地层中, 因此, 天山北部和西部形成的砂岩型铀矿床比其南部和东部的砂岩型铀矿床更多、更大(图1).

南亚的季节性季风气候在早中新世(24Ma)完全确立, 该地区降水量在15~12Ma达到峰值(Clift等, 2014). 在印度次大陆北部, 与印度-欧亚大陆碰撞有关的最早变形记录见于特提斯-喜马拉雅冲断带(Yin和Harrison, 2000). 该区域构造以南向的逆冲推覆为主, 即主要的中央逆冲推覆带(23~12Ma). 该区域向南的大规模逆冲作用使喜马拉雅前陆盆地的沉积地层发生倾斜, 包括Meghalaya高原(Yin等, 1994; Wesnousky等, 1999; Pearson和DeCelles, 2005). 早中新世中期, 青藏高原的海拔已达到>4km(Coleman和Hodges, 1995; Blisniuk等, 2001; Spicer等, 2003; Clift, 2006; Rowley和Currie, 2006; Wang C S等, 2014; Wang X等, 2014), 意味着, 自~22Ma开始, 青藏高原及其周边地区开始经历大规模的隆升与剥蚀(Coleman和Hodges, 1995; Armstrong和Allen, 2010). 青藏高原的形成改变了亚洲域内的大气环流模式, 并在夏季起到了空气泵的作用. 自始新世开始, 青藏高原在夏季吸引来自印度洋(印度洋季风)和太平洋(东亚夏季风)的潮湿空气(例如, 潘保田和李吉均, 1996; 吴国雄和张永生, 1998). 喜马拉雅山脉的快速隆升又阻挡了湿润的印度洋季风, 导致自早中新世开始(23~16Ma; Armstrong和Allen, 2010), 喜马拉雅山前开始出现大规模降水, 使靠近青藏高原的沉积地层经历快速剥蚀, 创造了将大气降水注入前陆盆地砂岩地层的条件(Boos和Kuang, 2010; 马耀明等, 2014). 这导致了Meghalaya高原上砂岩型铀矿床的形成.

东亚地区, 自始新世-渐新世开始, 区域年降水量逐渐升高(Clift, 2006), 并于早中新世(24~23Ma)达到峰值, 降水高峰期持续至约16Ma(Jiang和Ding, 2008). 从晚始新世到早中新世, 太平洋-欧亚板块的汇聚速度从50mm/a增加至80~90mm/a. 相比之下, 自晚始新世期开始, 印度-欧亚板块的汇聚速度一直保持在约50mm/a(Northrup等, 1995), 这可能反映了印度和欧亚大陆之间的强烈碰撞. 由陆内变形所导致的构造作用影响可能向北直至西伯利亚西部和南部, 导致西伯利亚南部和华北地区在晚渐新世-早中新世经历一期挤压变形(Delvaux等, 1995a, 1995b, 1995c, 2013). 太平洋板块向欧亚大陆之下俯冲的速度增加对华北-外贝加尔地区的构造影响也很重要(Zhang等, 2003; 索艳慧等, 2012; Niu等, 2015). 印度-欧亚大陆碰撞与太平洋板块的俯冲在欧亚大陆东部相互作用, 导致25Ma后主要山脉(包括燕山-阴山-大青山、太行山和六盘山山脉; Hilde等, 1977; Uyeda和Kanamori, 1979; Ma和Wu, 1987; Tian等, 1992)快速隆升, 最快的隆升发生在约20Ma. 这些山脉的快速隆升使内陆盆地边缘的地层倾斜, 砂岩地层出露. 在此期间, 东亚地区整体较为湿润, 大量的降水被注入内陆盆地的砂岩地层, 形成了众多的砂岩型铀矿床(Clift, 2006).

4.3　成矿第三阶段

砂岩型铀矿床大规模形成的最后一个阶段始于晚中新世(约8Ma). 由于印度次大陆持续向北挤压, 最终导致亚洲形成了目前的地貌格局(De Grave等, 2013; Burgette等, 2017). 在此期间, 中南半岛北部发育NW-SE走向的右旋走滑断层和N-S走向的正断层, 以应对青藏高原东部的顺时针旋转和快速隆升(Wang等, 1998; Cao等, 2011). 隆升导致西藏东部及周边地区开始经历快速剥蚀(Wang等, 2012; 王舫等, 2013).

砂岩型铀矿床年代学分析表明, 中亚地区部分砂岩型铀矿床非常年轻, 成矿年龄小于1Ma(如吐哈盆地, 伊犁盆地; Dahlkamp, 2009; Zhang和Liu, 2019). 这一阶段可能始于晚中新世, 由于印度板块向北持续挤压, 天山和阿尔泰山脉快速隆起所致(8~0Ma, Wang等(2015); 3~0Ma, Liu等(2017)). 天山北部和西部砂岩型铀矿床的成矿流体主要为春季和秋季大气降水(Caves等, 2017), 间接来源于亚洲西风. 作为对比, 天山内山间盆地或其南部和东部砂岩型铀矿床的成矿流体则主要来自于夏季大气降水和冰川融水(例如, Schiemann等, 2008, 2009; Baldwin和Vecchi, 2016; Zhang和Liu, 2019). 大气降水注入砂岩地层由重力驱动(Cuney和

Kyser, 2008; Cuney, 2010).

巴基斯坦的苏莱曼褶皱带(山脉, Szeliga等, 2012)是印度次大陆与阿富汗地块于上新世碰撞的直接结果(Treloar和Izatt, 1993). 该地区自5Ma开始经历快速隆升(Kassi等, 2009; Kasi等, 2012). 该阶段形成的砂岩型铀矿床产于不对称向斜中, 该向斜沿苏莱曼山脉东侧南北向延伸约300km. 发现的铀(和钒)矿化分别发生在潜水氧化面的上方和下方, 氧化和还原杂砂岩富含碳质片岩碎屑、黑云母和长石(Moghal, 1974a, 1974b, 1992, 2001). 与中亚砂岩型铀矿床的形成一样, 苏莱曼山脉阻挡了来自印度洋的湿润空气, 导致该地区出现季节性强降水. 砂岩地层的隆升和褶皱有利于大气降水的注入和砂岩型铀矿床的形成.

自晚中新世期开始, 中国华南地区遭受来自太平洋板块的构造挤压, 并且由于青藏高原向东的扩张, 导致华南地区发生顺时针旋转(Wang等, 1998). 华南西南边界断层(即哀牢山-红河剪切带)从右旋走滑变为左旋走滑(Ringin等, 1995). 华南地区的伸展构造可能是由于南海的扩张或山间盆地的隆升所导致的(Tapponnier等, 1982; Peltzer和Tapponnier, 1988; Li等, 2014a, 2014b). 自晚中新世开始, 华南地区亚洲季风开始加剧, 这意味着华南的降水量开始加大(An等, 2001). 自晚中新世期开始, 构造抬升和降水增强导致华南地区砂岩型铀矿床的形成.

蒙古高原和周围山脉最近经历了由印度-欧亚大陆碰撞的远程效应所导致的隆升(程绍平等, 2000; Walker等, 2007; Hunt等, 2012). 与第二阶段砂岩型铀矿床的形成类似, 该铀矿形成阶段对应亚洲季风的增强(An等, 2001; 汶玲娟等, 2004; Sun和Wang, 2005; Mirza, 2011).

5 结论

亚洲不同地区的砂岩型铀矿床具有相近的成矿年龄, 且与区域隆升事件和亚洲气候演化相吻合. 砂岩型铀矿化集中发生于温室气候和亚洲季风增强阶段(图2). 在温室气候阶段, 剧烈的海洋-大气环流会增加全球年降水量和蒸发量(例如, Linacre等, 1970; Gilman, 1994). 亚洲季风增强期间, 降水集中发生在特定季节. 此外, 温室气候阶段, 大气CO_2含量高于现在水平, 从而使大气降水酸性增强(例如, Royer等, 2004; Royer, 2016). 因此, 地下水从碎屑沉积物中提取铀的能力将比现在更强(例如, Almendinger, 1990; White和Buss, 2014). 地球的构造演化对区域气候产生重要影响(Manabe和Broccoli, 1990; Liu等, 2019), 如"水塔"效应, 以及隆起事件导致的山脉"雨影"效应, 在山麓地区形成大规模降水, 从而创造大量地表水注入砂岩地层的条件. 本文认为, 气候-构造的相互作用叠加在合适的盆地上, 导致了自晚中生代以来亚洲砂岩型铀矿床的大规模幕式爆发.

致谢 感谢池国祥教授、匿名审稿人和责任编委的建设性意见.

参考文献

陈正乐, 李丽, 刘健, 宫红良, 蒋荣宝, 李胜祥, 郑恩玖, 韩效忠, 李细根, 王成. 2008. 西天山隆升-剥露过程初步研究. 岩石学报, 24: 625–636

程绍平, 邓起东, 杨桂枝, 任殿卫. 2000. 内蒙古大青山的新生代剥蚀和隆起. 地震地质, 22: 27–36

程银行, 张天福, 曾威, 胡鹏, 刘行, 杨君, 曲凯, 王少轶, 程先钰, 奥琮, 金若时, 苗培森. 2020.中国北方中新生代盆地砂岩型铀超常富集的驱动力. 大地构造与成矿学, 44: 590–606

郭召杰, 张志诚, 吴朝东, 方世虎, 张锐. 2006. 中、新生代天山隆升过程及其与准噶尔、阿尔泰山比较研究. 地质学报, 80: 1–15

韩效忠, 张字龙, 姚春玲, 李西得, 李胜祥, 苗爱生, 杨建新. 2008. 鄂尔多斯盆地东北部砂岩型铀成矿模式研究. 矿床地质, 27: 415–422

黄净白, 黄世杰, 张金带, 李友良, 韩长青. 2005. 中国铀成矿带概论. 北京: 中国核工业地质局

姜必广, 沈赵明, 祝兵, 孙龙强, 黄绍琼. 2017. 衡阳盆地砂岩型铀矿地质特征与成矿模式——以汪家冲铀矿床为例. 铀矿地质, 33: 82–88

金若时, 程银行, 李建国, 司马献章, 苗培森, 王少轶, 奥琮, 里宏亮, 李艳锋, 张天福. 2017. 中国北方晚中生代陆相盆地红-黑岩系耦合产出对砂岩型铀矿成矿环境的制约. 中国地质, 44: 205–223

柳益群, 李继红, 冯乔, 陈法正, 邢秀娟, 樊爱萍. 2009. 鄂尔多斯盆地三叠-侏罗系的成岩作用及其成藏成矿响应. 岩石学报, 25: 2331–2339

吕红华, 常远, 王玮, 周祖翼. 2013. 天山中新世早期快速剥露: 磷灰石裂变径迹与(U-Th)/He低温热年代学证据. 中国科学: 地球科学, 43: 1964–1974

吕红华, 李有利, 刘运明, 司苏沛, 赵洪壮. 2008a. 新疆塔西河地区8Ma以来沉积环境演化及其构造意义. 第四纪研究, 28: 243–252

吕红华, 李有利, 南峰, 司苏沛, 刘运明, 钱莽, 赵红壮. 2008b. 天山北

麓河流阶地序列及形成年代. 地理学报, 63: 65–74
马耀明, 胡泽勇, 田立德, 张凡, 段安民, 阳坤, 张镱锂, 杨永平. 2014. 青藏高原气候系统变化及其对东亚区域的影响与机制研究进展. 地球科学进展, 29: 207–215
潘保田, 李吉均. 1996. 青藏高原: 全球气候变化的驱动机与放大器(III). 兰州大学学报: 自然科学版, 32: 108–115
索艳慧, 李三忠, 戴黎明, 刘鑫, 周立宏. 2012. 东亚及其大陆边缘新生代构造迁移与盆地演化. 岩石学报, 28: 2602–2618
陶君容, 杜乃秋. 1982. 云南腾冲新第三纪植物群及其时代. 植物学报, 24: 273–281
王舫, 刘福来, 刘平华. 2013. 点苍山-哀牢山变质杂岩带变沉积岩的变质演化. 岩石学报, 29: 630–640
王同和, 汪泽成, 赵宗举, 蔡希源, 王根海, 迟元林. 2001. 中国油气区反转构造. 北京: 石油工业出版社
汶玲娟, 鹿化煜, 强小科. 2004. 新近纪黄土高原红黏土粒度和沉积速率的空间变化及其揭示的古大气粉尘传输动力. 中国科学D辑: 地球科学, 34: 739–747
吴国雄, 张永生. 1998. 青藏高原的热力和机械强迫作用以及亚洲季风的爆发. I. 爆发地点. 大气科学, 22: 825–838
夏毓亮. 2019. 中国铀成矿年代学. 北京: 中国原子能出版社
张文高, 陈正乐. 2017. 西天山中新生代古高程恢复研究. 地球学报, 38: 69–72
中国核工业地质局, 核工业北京地质研究院. 2010. 中国砂岩型铀矿床研究评价. 北京: 中国核工业集团有限公司
Aizen E M, Aizen V B, Melack J M, Nakamura T, Ohta T. 2001. Precipitation and atmospheric circulation patterns at mid-latitudes of Asia. Int J Climatol, 21: 535–556
Alexandre P, Kyser K, Jiricka D, Witt G. 2012. Formation and evolution of the Centennial unconformity-related uranium deposit in the southcentral Athabasca Basin, Canada. Econ Geol, 107: 385–400
Alexandre P, Kyser K, Thomas D, Polito P, Marlat J. 2007. Geochronology of unconformity-related uranium deposits in the Athabasca Basin, Saskatchewan, Canada and their integration in the evolution of the basin. Miner Depos, 44: 41–59
Almendinger J E. 1990. Groundwater control of closed-basin lake levels under steady-state conditions. J Hydrol, 112: 293–318
An Z S, Kutzbach E J, Prell L W, Porter C S. 2001. Evolution of Asian monsoons and phased uplift of the Himalaya-Tibetan plateau since Late Miocene times. Nature, 411: 62–66
An Z S, Sun Y B, Chang H, Zhang P Z, Liu X D, Cai Y J, Jin Z D, Qiang X K, Zhou W J, Li L, Shi Z G, Tan L C, Li X Q, Zhang X B, Jin Z. 2014. Late Cenozoic climate change in monsoon-arid Asia and global changes. In: An Z S, ed. Late Cenozoic Climate Change in Asia. Berlin: Springer. 491–581
Anagnostou E, John E H, Edgar K M, Foster G L, Ridgwell A, Inglis G N, Pancost R D, Lunt D J, Pearson P N. 2016. Changing atmospheric CO_2 concentration was the primary driver of early Cenozoic climate. Nature, 533: 380–384
Armstrong H A, Allen M B. 2010. Shifts in the Intertropical Convergence Zone, Himalayan exhumation, and late Cenozoic climate. Geology, 39: 11–14
Baldwin J, Vecchi G. 2016. Influence of the Tian Shan on arid extratropical Asia. J Clim, 29: 5741–5762
Bice K L, Norris R D. 2002. Possible atmospheric CO_2 extremes of the Middle Cretaceous (late Albian-Turonian). Paleoceanography, 17: 22-1–22-17
Blisniuk P M, Hacker B R, Glodny J, Ratschbacher L, Bi S W, Wu Z H, McWilliams M O, Calvert A. 2001. Normal faulting in central Tibet since at least 13.5 Myr ago. Nature, 412: 628–632
Bonnetti C, Liu X D, Mercadier J L, Cuney M, Deloule E, Villeneuve J, Liu W Q. 2018. The genesis of granite-related hydrothermal uranium deposits in the Xiazhuang and Zhuguang ore fields, North Guangdong Province, SE China: Insights from mineralogical, trace elements and U-Pb isotopes signatures of the U mineralisation. Ore Geol Rev, 92: 588–612
Boos W R, Kuang Z. 2010. Dominant control of the South Asian monsoon by orographic insulation versus plateau heating. Nature, 463: 218–222
Boucot A J, Xu C, Scotese C R. 2013. Phanerozoic paleoclimate: An atlas of lithologic indicators of climate. In: Nichols G J, Ricketts B, eds. Concepts in Sedimentology and Paleontology. Tulsa: SEPM Society for Sedimentary Geology. 11: 478
Bowring S A, Erwin D H, Jin Y G, Martin M W, Davidek K, Wang W. 1998. U/Pb zircon geochronology and tempo of the End-Permian mass extinction. Science, 280: 1039–1045
Burgette R J, Weldon II R J, Abdrakhmatov K Y, Ormukov C, Owen L A, Thompson S C. 2017. Timing and process of river and lake terrace formation in the Kyrgyz Tien Shan. Quat Sci Rev, 159: 15–34
Burtman V S. 1975. Structural geology of variscan Tien Shan, USSR. Am J Sci, 275: 157–186
Buslov M M, Kokh D A, De Grave J. 2008. Mesozoic-Cenozoic tectonics and geodynamics of Altai, Tien Shan, and Northern Kazakhstan, from apatite fission-track data. Russ Geol Geophys, 49: 648–654
Cao S, Liu J, Leiss B, Neubauer F, Genser J, Zhao C. 2011. Oligo-Miocene shearing along the Ailao Shan-Red River shear zone: Constraints from structural analysis and zircon U/Pb geochronology of magmatic rocks in the Diancang Shan massif, SE Tibet, China. Gondwana Res, 19: 975–993
Cao X Z, Li S Z, Xu L Q, Guo L L, Liu L P, Zhao S J, Liu X, Dai L M.

2015. Mesozoic-Cenozoic evolution and mechanism of tectonic geomorphology in the central North China Block: Constraint from apatite fission track thermochronology. J Asian Earth Sci, 114: 41–53
Catlos E J, Harrison T M, Kohn M J, Grove M, Ryerson F J, Manning C E, Upreti B N. 2001. Geochronologic and thermobarometric constraints on the evolution of the Main Central Thrust, central Nepal Himalaya. J Geophys Res, 106: 16177–16204
Caves K J, Bayshashov U B, Zhamangara A, Ritch J A, Ibarra E D, Sjostrom J D, Mix T H, Winnick J M, Chamberlain C P. 2017. Late Miocene uplift of the Tian Shan and Altai and reorganization of central Asia climate. GSA Today, 27: 19–27
Caves K J. 2017. The Cenozoic climatic and tectonic history of Asia. Doctoral Dissertation. Stanford: Stanford University
Charreau J, Chen Y, Gilder S, Dominguez S, Avouac J P, Sen S, Sun D, Li Y, Wang W M. 2005. Magnetostratigraphy and rock magnetism of the Neogene Kuitun He section (northwest China): Implications for Late Cenozoic uplift of the Tianshan mountains. Earth Planet Sci Lett, 230: 177–192
Charreau J, Gilder S, Chen Y, Dominguez S, Avouac J P, Sen S, Jolivet M, Li Y G, Wang W M. 2006. Magnetostratigraphy of the Yaha section, Tarim Basin (China): 11 Ma acceleration in erosion and uplift of the Tian Shan mountains. Geology, 34: 181–184
Charreau J, Gumiaux C, Avouac J P, Augier R, Chen Y, Barrier L, Gilder S, Dominguez S, Charles N, Wang Q C. 2009. The Neogene Xiyu Formation, a diachronous prograding gravel wedge at front of the Tianshan: Climatic and tectonic implications. Earth Planet Sci Lett, 287: 298–310
Chen F H, Chen J H, Huang W, Chen S Q, Huang X Z, Jin L Y, Jia J, Zhang X J, An C B, Zhang J W, Zhao Y, Yu Z C, Zhang R H, Liu J B, Zhou A F, Feng S. 2019. Westerlies Asia and monsoonal Asia: Spatiotemporal differences in climate change and possible mechanisms on decadal to sub-orbital timescales. Earth-Sci Rev, 192: 337–354
Chen J, Bever G S, Yi H Y, Norell M A. 2016. A burrowing frog from the late Paleocene of Mongolia uncovers a deep history of spadefoot toads (Pelobatoidea) in East Asia. Sci Rep, 6: 19209
Chen K, Lin W, Wang Q C. 2015. The Bogeda Shan uplifting: Evidence from multiple phases of deformation. J Asian Earth Sci, 99: 1–12
Chen X Q, Chi Z Q, Dong S W, Yan Z, Yang J S, Shi W, Min L R, Wang Y, Yao P Y. 2015. Late Cenozoic sedimentation of Nihewan Basin, central North China and its tectonic significance. J Asian Earth Sci, 114: 242–257
Cheng Y H, Wang S Y, Jin R S, Li J G, Ao C, Teng X M. 2019. Global Miocene tectonics and regional sandstone-style uranium mineralization. Ore Geol Rev, 106: 238–250
Cheng Y H, Wang S Y, Zhang T F, Teng X M, Ao C, Jin R S, Li H L. 2020. Regional sandstone-type uranium mineralization rooted in Oligo-Miocene tectonic inversion in the Songliao Basin, NE China. Gondwana Res, 88: 88–105
Clemens S. 2006. Extending the historical record by proxy. In: Wang B, ed. The Asian Monsoon. Berlin: Springer Praxis Books. 615–630
Clift P D, Webb A A G. 2019. A history of the Asian monsoon and its interactions with solid Earth tectonics in Cenozoic South Asia. Geol Soc Lond Spec Publ, 483: 631–652
Clift P D, Wan S, Blusztajn J. 2014. Reconstructing chemical weathering, physical erosion and monsoon intensity since 25 Ma in the northern South China Sea: A review of competing proxies. Earth-Sci Rev, 130: 86–102
Clift P D. 2006. Controls on the erosion of Cenozoic Asia and the flux of clastic sediment to the ocean. Earth Planet Sci Lett, 241: 571–580
Coleman M, Hodges K. 1995. Evidence for Tibetan plateau uplift before 14 Myr ago from a new minimum age for east-west extension. Nature, 374: 49–52
Crumley C. 2004. The Little Ice Age: How climate made history 1300–1850. Am Antiq, 69: 186–187
Cuney M, Kyser K. 2008. Recent and not-so-recent developments in uranium deposits and implications for exploration. Mineral Assoc Can, 39: 161–219
Cuney M. 2010. Evolution of uranium fractionation processes through time: Driving the secular variation of uranium deposit types. Econ Geol, 105: 553–569
Curio J, Maussion F, Scherer D. 2015. A 12-year high-resolution climatology of atmospheric water transport over the Tibetan Plateau. Earth Syst Dynam, 6: 109–124
Dahlkamp J F. 2009. Uranium Deposits of the World (Asia Part). Berlin Heidelberg: Springer-Verlag. 1–509
Dahlkamp J F. 2010. Uranium Deposits of the World (USA and Latin Amercia). Berlin Heidelberg: Springer-Verlag. 1–536
Dahlkamp J F. 2016. Uranium Deposits of the World (Europe). Berlin Heidelberg: Springer-Verlag. 1–800
Davis W D, Williams S I, Krogh E T. 2003. Historical development of zircon geochronology. Rev Mineral Geochem, 53: 145–181
Davy P, Cobbold P R. 1988. Indentation tectonics in nature and experiment. 1. Experiments scaled for gravity. Bull Geol Inst Upp New Series, 14: 129–141
Delvaux D, Cloetingh S, Beekman F, Sokoutis D, Burov E, Buslov M M, Abdrakhmatov K E. 2013. Basin evolution in a folding lithosphere: Altai-Sayan and Tien Shan belts in Central Asia. Tectonophysics, 602: 194–222
Delvaux D, Fernandez-Alonso M, Klerkx J, Kuzmin A, Matton C,

Selegei V, Theunissen K, Vysotskii E. 1995a. Evidences for active tectonics in Lake Teletskoye (Gorny-Altai, South-Siberia). Russ Geol Geophys, 36: 100–112

Delvaux D, Moeys R, Stapel G, Melnikov A, Ermikov V. 1995b. Palaeostress reconstructions and geodynamics of the Baikal region, Central Asia, Part I. Palaeozoic and Mesozoic pre-rift evolution. Tectonophysics, 252: 61–101

Delvaux D, Theunissen K, Van der Meer R, Berzin N. 1995c. Formation dynamics of the Gorno-Altaian Chuya-Kurai depression in Southern Siberia: Paleostress, tectonic and climatic control. Russ Geol Geophys, 36: 26–45

Faure G. 1977. Principles of Isotope Geology. New York: John Wiley & Sons. 146–209

Fayek M, Harrison T M, Grove M, Coath C D. 2000. A rapid *in situ* method for determining the ages of uranium oxide minerals: Evolution of the Cigar Lake Deposit, Athabasca Basin. Int Geol Rev, 42: 163–171

Fournier M, Jolivet L, Davy P, Thomas J C. 2004. Backarc extension and collision: An experimental approach to the tectonics of Asia. Geophys J Int, 157: 871–889

Friedrich T, Timmermann A, Abe-Ouchi A, Bates N R, Chikamoto M O, Church M J, Dore J E, Gledhill D K, González-Dávila M, Heinemann M, Ilyina T, Jungclaus J H, McLeod E, Mouchet A, Santana-Casiano J M. 2012. Detecting regional anthropogenic trends in ocean acidification against natural variability. Nat Clim Change, 2: 167–171

Fyodorov G V. 2002a. A comparative description of the geological-technological description of the sandstone hosted uranium deposits in Wyoming and southern Kazakhstan. Vienna: IAEA. T1-TC-975: 42–48

Fyodorov G V. 2002b. Uranium production and the environment in Kazakhstan. CandS Papers Series, The Uranium Production Cycle and the Environment. Vienna: IAEA. 191–198

Gao Y, Ibarra E D, Wang C S, Caves K J, Chamberlain P C, Graham A S, Wu H C. 2015. Mid-latitude terrestrial climate of East Asia linked to global climate in the Late Cretaceous. Geology, 43: 287–290

Gilman K. 1994. Hydrology and Wetland Conservation. Chichester: Wiley

De Grave J, Glorie S, Buslov M M, Stockli D F, McWilliams M O, Batalev V Y, Van den haute P. 2013. Thermo-tectonic history of the Issyk-Kul basement (Kyrgyz Northern Tien Shan, Central Asia). Gondwana Res, 23: 998–1020

Groves D I, Condie K C, Goldfarb R J, Hronsky J M A, Vielreicher R M. 2005. Secular changes in global tectonic processes and their influence on the temporal distribution of gold-bearing mineral deposits. Econ Geol, 100: 203–224

Gu C G, Renaut R W. 1994. The effect of Tibetan uplift on the formation and preservation of Tertiary lacustrine source-rocks in eastern China. J Paleolimnol, 11: 31–40

Guo Z T, Sun B, Zhang Z S, Peng S Z, Xiao G Q, Ge J Y, Hao Q Z, Qiao Y S, Liang M Y, Liu J F, Yin Q Z, Wei J J. 2008. A major reorganization of Asian climate by the early Miocene. Clim Past, 4: 153–174

Harrison T M, Copeland P, Kidd W S F, Yin A. 1992. Raising Tibet. Science, 255: 1663–1670

Hilde T W C, Uyeda S, Kroenke L. 1977. Evolution of the western pacific and its margin. Tectonophysics, 38: 145–165

Hong H J, Bae C J, Zhang Z S. 2018. Cenozoic climate change in eastern Asia: Part I. Palaeogeogr Palaeoclimatol Palaeoecol, 510: 1–5

Huber M, Goldner A. 2012. Eocene monsoons. J Asian Earth Sci, 44: 3–23

Hunt A C, Parkinson I J, Harris N B W, Barry T L, Rogers N W, Yondon M. 2012. Cenozoic volcanism on the Hangai Dome, Central Mongolia: Geochemical evidence for changing melt sources and implications for mechanisms of melting. J Petrol, 53: 1913–1942

Jiang H C, Ding Z L. 2008. A 20 Ma pollen record of East-Asian summer monsoon evolution from Guyuan, Ningxia, China. Palaeogeogr Palaeoclimatol Palaeoecol, 265: 30–38

Jiang W Y, Leroy S A G, Ogle N, Chu G, Luo W, Liu J. 2008. Natural and anthropogenic forest fires recorded in the Holocene pollen record from a Jinchuan peat bog, northeastern China. Palaeogeogr Palaeoclimatol Palaeoecol, 261: 47–57

Jin R S, Liu H J, Li X G. 2022. Theoretical system of sandstone-type uranium deposits in northern China. J Earth Sci, 33: 257–277

Jin R S, Teng X M, Li X G, Si Q H, Wang W. 2020. Genesis of sandstone-type uranium deposits along the northern margin of the Ordos Basin, China. Geosci Front, 11: 215–227

Kasi A K, Kassi A M, Umar M, Manan R A. 2012. Revised lithostratigraphy of the Pishin Belt, northwestern Pakistan. J Himalayan Earth Sci, 45: 53–65

Kassi A M, Kelling G, Kasi A K, Umar M, Khan A S. 2009. Contrasting Late Cretaceous-Palaeocene lithostratigraphic successions across the Bibai Thrust, western Sulaiman Fold-Thrust Belt, Pakistan: Their significance in deciphering the early-collisional history of the NW Indian Plate margin. J Asian Earth Sci, 35: 435–444

Koons P O, Zeitler P K, Chamberlain C P, Craw D, Meltzer A S. 2002. Mechanical links between erosion and metamorphism in Nanga Parbat, Pakistan Himalaya. Am J Sci, 302: 749–773

Li J H, Ma Z L, Zhang Y Q, Dong S W, Li Q, Lu M A, Tan J Q. 2014a. Tectonic evolution of Cretaceous extensional basins in Zhejiang

Province, eastern South China: Structural and geochronological constraints. Int Geol Rev, 56: 1602–1629
Li J H, Zhang Y Q, Dong S W, Johnston S T. 2014b. Cretaceous tectonic evolution of South China: A preliminary synthesis. Earth-Sci Rev, 134: 98–136
Li S Z, Zhao G C, Dai L M, Liu X, Zhou L H, Santosh M, Suo Y H. 2012a. Mesozoic basins in eastern China and their bearing on the deconstruction of the North China Craton. J Asian Earth Sci, 47: 64–79
Li S Z, Zhao G C, Dai L M, Zhou L H, Liu X, Suo Y H, Santosh M. 2012b. Cenozoic faulting of the Bohai Bay Basin and its bearing on the destruction of the eastern North China Craton. J Asian Earth Sci, 47: 80–93
Linacre E T, Hicks B B, Sainty G R, Grauze G. 1970. The evaporation from a swamp. Agric Meteorol, 7: 375–386
Liu D L, Li H B, Sun Z M, Cao Y, Wang L Z, Pan J W, Han L, Ye X Z. 2017. Cenozoic episodic uplift and kinematic evolution between the Pamir and Southwestern Tien Shan. Tectonophysics, 712-713: 438–454
Liu X D, Dong B W, Yin Z Y, Smith S R, Guo Q C. 2019. Continental drift, plateau uplift, and the evolutions of monsoon and arid regions in Asia, Africa, and Australia during the Cenozoic. Sci China Earth Sci, 62: 1053–1075
Ludwig K R, Nash J T, Naeser C W. 1981. U-Pb isotope systematics and age of uranium mineralization, Midnite Mine, Washington. Econ Geol, 76: 89–110
Ludwig K R, Simmons K R, Webster J D. 1984. U-Pb isotope systematics and apparent ages of uranium ores, Ambrosia Lake and Smith Lake districts, Grants mineral belt, New Mexico. Econ Geol, 79: 322–337
Ludwig K R, Simmons K R. 1992. U-Pb dating of uranium deposits in collapse breccia pipes of the Grand Canyon region. Econ Geol, 87: 1747–1765
Ludwig K R. 1978. Uranium-daughter migration and U/Pb isotope apparent ages of uranium ores, Shirley Basin, Wyoming. Econ Geol, 73: 29–49
Ludwig K R. 1980. Calculation of uncertainties of U-Pb isotope data. Earth Planet Sci Lett, 46: 212–220
Ludwig K R. 1984. PBDAT-a program for reduction of Pb-U-Th isotope data, for use with HP-86/87 microcomputers. Open-File Report. U.S.Geol. Survey. 83–113: 54
Ludwig K R. 1993. ISOPLOT: A plotting and regression program for radiogenic-isotope data. Open File Report: U.S. Geological Survey. 91–445: 1–42
Ludwig R K, Wallace R A, Simmons R K. 1985. The Schwartzwalder uranium deposit; II, Age of uranium mineralization and lead isotope constraints on genesis. Econ Geol, 80: 1858–1871
Ma X Y, Wu D N. 1987. Cenozoic extensional tectonics in China. Tectonophysics, 133: 243–255
Malavieille J. 2010. Impact of erosion, sedimentation, and structural heritage on the structure and kinematics of orogenic wedges: Analog models and case studies. GSA Today, 20: 4–10
Manabe S, Broccoli A J. 1990. Mountains and arid climates of middle latitudes. Science, 247: 192–195
Mercier J L, Vergely P, Zhang Y Q, Hou M J, Bellier O, Wang Y M. 2013. Structural records of the Late Cretaceous-Cenozoic extension in Eastern China and the kinematics of the Southern Tan-Lu and Qinling Fault Zone (Anhui and Shaanxi provinces, PR China). Tectonophysics, 582: 50–75
Meyer-Christoffer A, Becker A, Finger P, Rudolf B, Schneider U, Ziese M. 2015. GPCC Climatology Version 2015 at 0.25°: Monthly Land-Surface Precipitation Climatology for Every Month and the Total Year from Rain-Gauges built on GTS-based and Historic Data
Mirza M M Q. 2011. Climate change, flooding in South Asia and implications. Reg Environ Change, 11: 95–107
Moghal M Y. 1974a. Uranium in Siwalik sandstones, Sulaiman Range, Pakistan. In: Formation of uranium ore deposits. Vienna: IAEA. 383–400
Moghal M Y. 1974b. Exploration of uranium deposits in Dera Ghazi Khan District (Punjab), Pakistan. Quetta Geol Surv Pak Geonews, 5: 72–78
Moghal M Y. 1992. Field test for *in situ* leach mining of uranium in Pakistan. In: New developments in uranium exploration, resources, production and demand. Vienna: IAEA. TECDOC-650: 214–224
Moghal M Y. 2001. Current uranium activities in Pakistan. In: Assessment of uranium deposit types and resources—A worldwide perspective. Vienna: IAEA. TECDOC-1258: 101–115
Molnar P, Tapponnier P. 1975. Cenozoic Tectonics of Asia: Effects of a Continental Collision: Features of recent continental tectonics in Asia can be interpreted as results of the India-Eurasia collision. Science, 189: 419–426
Niu Y L, Liu Y, Xue Q Q, Shao F L, Chen S, Duan M, Guo P Y, Gong H M, Hu Y, Hu Z X, Kong J J, Li J Y, Liu J J, Sun P, Sun W, Ye L, Xiao Y Y, Zhang Y. 2015. The exotic origin of the continental shelf of East and South China Seas-A testable hypothesis with consequences on the tectonic evolution of the western Pacific and eastern China since the Mesozoic. Sci Bull, 60: 1598–1616
Northrup C J, Royden L H, Burchfiel B C. 1995. Motion of the Pacific plate relative to Eurasia and its potential relation to Cenozoic extension along the eastern margin of Eurasia. Geology, 23: 719–722
OECD-NEA/IAEA. 2014. Uranium 2014: Resources, Production and

Demand
Pagel M, Cavellec S, Forbes P, Gerbaut O, Vergely P, Wagani I, Mathieu R. 2005. Uranium deposits in the Arlit area (Niger). Beijing: Proceedings of the Eighth Biennial SGA Meeting, 2005. 303–305
Pearson O N, DeCelles P G. 2005. Structural geology and regional tectonic significance of the Ramgarh thrust, Himalayan fold-thrust belt of Nepal. Tectonics, 24
Peltzer G, Tapponnier P. 1988. Formation and evolution of strike-slip faults, rifts, and basins during the India-Asia Collision: An experimental approach. J Geophys Res, 93: 15085–15117
Petrov N N, Yazikov V G, Berikbolov B R, Vershkov A F, Egorov S A, Zhelnov V P, Karelin V G, Kravtsov E G, Nikolaev S L, Ostrokom I M, Shishkov I A. 2000. Uranium deposits of Kazakhstan (endogenous) (in Russian). Gylym Almaty, 400–523
Petrov N N. 1998. Epigenetic stratified-infiltration uranium deposits of Kazakhstan (in Russian). Geol Kazakhstan, 2: 22–39
Phillips F M, Castro M C. 2014. Groundwater dating and residence-time measurements. In: Holland H D, Turekian K K, eds. Treatise on Geochemistry. Oxford: Elsevier. 362–377
Raymo M E, Ruddiman W F. 1992. Tectonic forcing of late Cenozoic climate. Nature, 359: 117–122
Ringin C, Klein M, Roques D, Le P X, Van Trong L. 1995. The Red River fault system in the Tonkin Gulf, Vietnam. Tectonophysics, 243: 209–222
Robb L J. 2005. Introduction to Ore-Forming Processes. Oxford: Blcakwell Publishing Company. 311–325
Roe G H, Ding Q, Battisti D S, Molnar P, Clark M K, Garzione C N. 2016. A modeling study of the response of Asian summertime climate to the largest geologic forcings of the past 50 Ma. J Geophys Res-Atmos, 121: 5453–5470
Rollinson H. 1994. Using Geochemical Data: Evolution, Presentation, Interpretation. England, Essex: Longman Scientific & Technical. 15–258
Rowley D B, Currie B S. 2006. Palaeo-altimetry of the late Eocene to Miocene Lunpola basin, central Tibet. Nature, 439: 677–681
Royer D L, Berner R A, Montañez I P, Tabor N J, Beerling D J. 2004. CO_2 as a primary driver of Phanerozoic climate. GSA Today, 14: 4–10
Royer D L. 2016. Climate sensitivity in the geologic past. Annu Rev Earth Planet Sci, 44: 277–293
Sato T, Tsujimura M, Yamanaka T, Iwasaki H, Sugimoto A, Sugita M, Kimura F, Davaa G, Oyunbaatar D. 2007. Water sources in semiarid northeast Asia as revealed by field observations and isotope transport model. J Geophys Res, 112: D17112
Schiemann R, Lüthi D, Schär C. 2009. Seasonality and interannual variability of the westerly jet in the Tibetan Plateau region. J Clim, 22: 2940–2957
Schiemann R, Lüthi D, Vidale P L, Schär C. 2008. The precipitation climate of Central Asia—Intercomparison of observational and numerical data sources in a remote semiarid region. Int J Climatol, 28: 295–314
Spicer R A, Harris N B W, Widdowson M, Herman A B, Guo S, Valdes P J, Wolfe J A, Kelley S P. 2003. Constant elevation of southern Tibet over the past 15 million years. Nature, 421: 622–624
Sun J M, Windley B F. 2015. Onset of aridification by 34 Ma across the Eocene-Oligocene transition in Central Asia. Geology, 43: 1015–1018
Sun X J, Wang P X. 2005. How old is the Asian monsoon system?—Palaeobotanical records from China. Palaeogeogr Palaeoclimatol Palaeoecol, 222: 181–222
Szeliga W, Bilham R, Kakar D M, Lodi S H. 2012. Interseismic strain accumulation along the western boundary of the Indian subcontinent. J Geophys Res, 117
Tapponnier P, Peltzer G, Le Dain A Y, Armijo R, Cobbold P. 1982. Propagating extrusion tectonics in Asia: New insights from simple experiments with plasticine. Geology, 10: 611–616
Thomas W A. 2011. Detrital-zircon geochronology and sedimentary provenance. Lithosphere, 3: 304–308
Tian Z Y, Han P, Xu K D. 1992. The Mesozoic-Cenozoic East China rift system. Tectonophysics, 208: 341–363
Treloar P J, Izatt C N. 1993. Tectonics of the Himalayan collision between the Indian Plate and the Afghan Block: A synthesis. Geol Soc Lond Spec Publ, 74: 69–87
Uyeda S, Kanamori H. 1979. Back-arc opening and the mode of subduction. J Geophys Res, 84: 1049–1061
Walker R T, Nissen E, Molor E, Bayasgalan A. 2007. Reinterpretation of the active faulting in central Mongolia. Geology, 35: 759–762
Wang C S, Dai J G, Zhao X X, Li Y L, Graham S A, He D F, Ran B, Meng J. 2014. Outward-growth of the Tibetan Plateau during the Cenozoic: A review. Tectonophysics, 621: 1–43
Wang E, Kirby E, Furlong K P, van Soest M, Xu G, Shi X, Kamp P J J, Hodges K V. 2012. Two-phase growth of high topography in eastern Tibet during the Cenozoic. Nat Geosci, 5: 640–645
Wang M, Zhang J J, Liu K. 2015. Continuous denudation and pediplanation of the Chinese Western Tianshan orogen during Triassic to Middle Jurassic: Integrated evidence from detrital zircon age and heavy mineral chemical data. J Asian Earth Sci, 113: 310–324
Wang P L, Lan C Y, Yem N T, Lo C H, Lee T Y, Chung S L. 1998. Thermochronological evidence for the movement of the Ailao Shan-Red River shear zone: A perspective from Vietnam. Geology, 26:

887–890
Wang X, Sun D H, Chen F H, Wang F, Li B F, Popov S V, Wu S, Zhang Y B, Li Z J. 2014. Cenozoic paleo-environmental evolution of the Pamir-Tien Shan convergence zone. J Asian Earth Sci, 80: 84–100
Wesnousky S G, Kumar S, Mohindra R, Thakur V C. 1999. Uplift and convergence along the Himalayan Frontal Thrust of India. Tectonics, 18: 967–976
White A F, Buss H L. 2014. Natural weathering rates of silicate Minerals. In: Holland H D, Turekian K K, eds. Treatise on Geochemistry. Oxford: Elsevier. 7: 116–151
Yang Y T. 2013. An unrecognized major collision of the Okhotomorsk Block with East Asia during the Late Cretaceous, constraints on the plate reorganization of the Northwest Pacific. Earth-Sci Rev, 126: 96–115
Yapp C J, Poths H. 1996. Carbon isotopes in continental weathering environments and variations in ancient atmospheric CO_2 pressure. Earth Planet Sci Lett, 137: 71–82
Yin A, Harrison T M. 2000. Geologic evolution of the Himalayan-Tibetan orogeny. Annu Rev Earth Planet Sci, 28: 211–280
Yin A, Harrison T, Ryerson F, Chen W, Kidd W, Copeland P. 1994. Tertiary structural evolution of the Gangdese thrust system, southeastern Tibet. J Geophys Res, 99: 18175–18201
Yin A. 2010. Cenozoic tectonic evolution of Asia: A preliminary synthesis. Tectonophysics, 488: 293–325
Zachos J, Pagani M, Sloan L, Thomas E, Billups K. 2001. Trends, rhythms, and aberrations in global climate 65 Ma to present. Science, 292: 686–693
Zhang C, Liu H X. 2019. A growing sandstone type uranium district in South Yili Basin, NW China as a result of extension of Tien Shan Orogen: Evidences from geochronology and hydrology. Gondwana Res, 76: 146–172
Zhang C, Yi C, Dong Q, Cai Y Q, Liu H X. 2018. Geological and geochronological evidence for the effect of Paleogene and Miocene uplift of the Northern Ordos Basin on the formation of the Dongsheng uranium district, China. J Geodyn, 114: 1–18
Zhang J D, Chen X H, Li Q L, Liu C Z, Li B, Li J, Liu G, Ren F L. 2012. Mesozoic “red beds” and its evolution in the Hefei Basin. Acta Geol Sin-Eng Ed, 86: 1060–1076
Zhang Q Q, Smith T, Yang J, Li C S. 2016. Evidence of a cooler continental climate in East China during the warm Early Cenozoic. PLoS One, 11: E0155507
Zhang Y Q, Shi W, Dong S W. 2011. Changes of Late Mesozoic tectonic regimes around the Ordos Basin (North China) and their geodynamic implications. Acta Geol Sin-Engl Ed, 85: 1254–1276
Zhang Y Q, Ma Y S, Yang N, Shi W, Dong S W. 2003. Cenozoic extensional stress evolution in North China. J Geodyn, 36: 591–613

(责任编委: 陈华勇)